ORIGINAL PAPER

Oxidation mechanism in the metabolism of (S)-N-[1-(3-morpholin-4-ylphenyl)ethyl]-3-phenylacrylamide on oxyferryl active site in CYP3A4 Cytochrome: DFT modeling

**Abdul Rajjak Shaikh · Ewa Broclawik ·
Hideyuki Tsuboi · Michihisa Koyama · Akira Endou ·
Hiromitsu Takaba · Momoji Kubo ·
Carlos A. Del Carpio · Akira Miyamoto**

Abstract The metabolism mechanism of (S)-N-[1-(3-mor-pholin-4ylphenyl)ethyl]-3-phenylacrylamide, mediated by CYP3A4 Cytochrome has been investigated by density functional QM calculations aided with molecular mechanics/molecular dynamics simulations. Two different orientations of phenyl ring for substrate approach toward oxyferryl center, imposing two subsequent rearrangement pathways have been investigated. Starting from σ-complex in perpendicular orientation enzymatic mechanism involves consecutive proton shuttle intermediate, which further leads to the formation of alcohol and ketone. Parallel conformation leads solely to ketone product by 1,2 hydride shift. Although parallel and perpendicular σ-complexes are energetically equivalent both for the gas phase or PCM solvent model, molecular dynamics studies in full CYP3A4 environment show that perpendicular conformation of the σ-complex should be privileged, stabilized by hydrophobic interactions of phenylacrylamide chain. After assessing probability of the two conformations we postulate that the alcohol, accessible with the lowest energy barriers should be the major metabolite for studied substrate and CYP3A4 enzyme.

A. R. Shaikh · H. Tsuboi · M. Koyama · A. Endou · H. Takaba ·
M. Kubo · C. A. Del Carpio · A. Miyamoto
Department of Applied Chemistry,
Graduate School of Engineering, Tohoku University,
6-6-07 Aoba, Aramaki, Aoba-ku,
Sendai 980-8579, Japan

E. Broclawik (✉)
Institute of Catalysis, Polish Academy of Sciences,
ul. Niezapominajek 8,
Kraków 30-239, Poland
e-mail: broclawi@chemia.uj.edu.pl

M. Kubo
PRESTO, Japan Science and Technology Agency,
4-1-8 Honcho, Kawaguchi,
Saitama 332-0012, Japan

A. Miyamoto
New Industry Creation Hatchery Centre, Tohoku University,
6-6-10 Aoba, Aramaki, Aoba-ku,
Sendai 980-8579, Japan

Introduction

The cytochrome P450 (CYP) [1] enzymes are membrane bound proteins that catalyze primary oxidations of endo-biotics and xenobiotics. CYP3A4 [2] is a major CYP450 isoform and contributes extensively to human drug metabolism due to its high level of expression in liver and broad capacity to oxidize structurally diverse substrates. It metabolizes 50% of drugs used in human being. Hydroxylation of the C-H bond of the drug is one of the most important metabolism steps that can influence their bio-availability by transforming them either to active form or to toxic compounds [3, 4]. A detailed understanding of this metabolism step and prediction of metabolites is thus a major challenge being crucial to screen drugs in early stage of lead development. Since experimental investigation of the catalytically competent species in the metabolism requires already the presence of a substrate to initiate the reaction cycle, computational methods are very important to accomplish this task. Such techniques involve docking in the active site, pharmacophore modeling, quantitative

structure activity relationship (QSAR) and/or quantum chemical/molecular mechanical (QM/MM) studies [5, 6]. Apart from practical significance, the recognition of the mechanism making enzymatic oxidation highly potent tool capable of activating the inert C-H bond in hydrocarbons, is itself of high scientific interest and deserves attention.

In this paper we focus on the compound (S)-N-[1-(3-morpholin-4-yl phenyl)ethyl]-3-phenylacrylamide (**1**) (Fig. 1), the novel KCNQ2 potassium channel opener that was found to have significant oral activity in a cortical spreading depression model of migraine [7, 8]. Substrate **1** has excellent oral bioavailability in dogs and rats; however, CYP3A4 MDI studies indicated that it forms reactive intermediate after metabolism. On the other hand, its difluoro analogue, (S)-N-[1-(4-fluoro-3-morpholin-4-yl phenyl)ethyl]-3-(4-fluorophenyl)acrylamide (Figs. 1, 2) was found to be orally bioavailable KCNQ2 opener free of CYP3A4 MDI [8]. The existence of a pair of closely related compounds with different MDI properties provides promising material and good guidance for examining details of selected steps in their metabolism; it also confirms the position of primary oxidation of phenyl ring.

The crystal structures of CYP3A4 both unbound and bound with substrates have been solved recently and the data are stored in PDB with entry codes 1W0E, 1W0F, 1W0G, 1TQN, 2J0C and 2J0D [9–11]. The active site of CYP3A4 is relatively large compared with other CYPs and can metabolize large ligands, the enzyme has been shown to process a broad variety of substrates, in addition its active site is remarkably flexible [1, 9–11]. Hence full prediction of drug-CYP3A4 interaction is difficult despite an exceptionally large amount of experimental and theoretical work devoted to understanding the pattern of the CYP reaction cycle. These two factors, interest focused on novel drug molecules with variable metabolism-dependent inhibition factor and the presence of many question marks in general reaction mechanism, prompted us to undertake this study. Our aim was also to verify how substituents in the phenyl fragment, transforming the molecule into actual drug-like structure, affect the metabolism.

Since the advent of a robust computational techniques based on density functional theory (DFT) quantum mechanical modeling has provided extensive information on catalytic cycle of cytochromes. This included transformation of the initial, inactive form of the enzyme into the active oxyferryl form, model ligand binding and subsequent metabolism. Recently a few comprehensive reviews have been published on the subject [12–14]. Doubts concerning hydroxylation step, however, are far from full resolution and the target substrate of this study (**1**) has not yet been examined at the molecular level by QM calculations. From comparative mechanistic considerations it is believed to metabolize mainly by hydroxylation of the phenyl ring in N-phenylmorpholine moiety following the arene hydroxylation mechanism. Our study is based on the accepted model of the oxidized active site bound with the substrate and focuses on its transformation. Here DFT calculations for a gas phase model composed of the active oxyferryl Compound I (Cpd I) form of the iron- porphyrin site [12–15] and the substrate molecule **1** (Fig. 1) are reported. DFT calculations are aided with continuum solvent model to mimic the polarizing effects of the protein environment [16, 17]. We comply with generally accepted opinion that aryl carbon hydroxylation proceeds primarily via the formation of a strong σ-complex followed by a proton shuttle mediated by a porphyrin, however, other possible reaction routes have also been considered and tested by calculating prospective intermediates.

A model for gas-phase QM is a cutoff from the CYP3A4 crystal structure after docking the substrate and auxiliary MD simulation for the oxidized, oxyferryl form. Analogous model has been explored by us [18] in the study of Cpd I addition to aryl carbon in substrate **1**. In our previous paper we have studied σ-complex formation, agreed to be the rate determining step in aromatic oxidation. In accord with other studies [19–21], the reaction proceeded on the doublet potential energy surface via the transition state with predominantly carbocationic character. On the contrary, the energy barrier of 7.4 kcal mol^{-1} for σ-complex formation with **1** in [18] was well below that reported earlier for benzene (15–17 kcal mol^{-1}) [19–21]. We have attributed significant lowering of the energy barrier for σ-complex with substrate **1** to the formation of a conjugated double bond with morpholine nitrogen in ortho position that should compensate the loss of aromatic stabilization. Here we extend our studies to consecutive transformations starting from the σ-complex. In our gas-phase modeling we have found two distinct conformations of the substrate σ-bonded to the oxyferryl oxygen: with parallel or perpendicular orientation between phenyl ring and the porphyrin. As both conformations were energetically equivalent, in
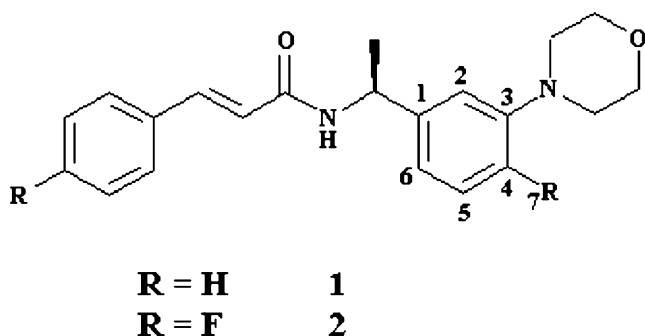

Fig. 1 Chemical structure of (S)-N-[1-(3-morpholin-4-ylphenyl)ethyl]-3-phenylacrylamide (**1**) and its difluoro analogue (**2**) (atoms important for metabolism mechanism labeled)

this article we present mechanistic considerations for subsequent rearrangement pathways for the formation of the alcohol and/or ketone starting from the two orientations. Possibility of epoxide formation is excluded here for substrate **1** as energetically unfavorable and sterically hindered. After qualitative assessing probability of the two conformations in a protein environment from auxiliary MD studies we postulate that the alcohol should be the highly privileged metabolite in the case of substrate **1** and CYP3A4. Thus we pinpoint the roles of both viable positioning of the substrate by hydrophobic interactions of the side chain with enzymatic cavity and the presence of substituents lowering the barrier for the rate determining step. Brief comparison with complementary modeling for fluoro-substituted substrate confirms both the position of the assumed primary hydroxylation site and the MDI blocking effect of fluorine substitution.

Methods and models

Docking, MD and visualization

Docking studies were carried out using the LigandFit [22–24] module incorporated in Cerius^2 for the active site of CYP3A4 crystal structure (PDB code: 1W0G) [9]. Energy minimization studies were performed using the Discover program in INSIGHT II (MSI/Accelrys, San Diego, USA) for 0.05 kcal mol^{-1} gradient with consistent valence force field (CVFF) modified to include parameters for heme and oxyferryl [25].

The most stable CYP3A4-substrate 1 complex obtained by docking studies and further minimized to remove bad steric contacts was used as an input structure for subsequent molecular dynamics (MD) simulations after adding oxyferryl oxygen. MD simulations were done using New-Ryudo program developed in our laboratory [26–29]. The Verlet algorithm was used for the calculation of the atomic motions and the Ewald method was applied for the calculations of the electrostatic interactions. The potential cut-off distance was 15 Å for short-range interaction and for the real part of the Ewald summation. Temperature was controlled by means of scaling the atomic velocities. CVFF force field was used with modified parameters for heme and oxyferryl heme [25]. MD simulations were carried out with periodic boundary conditions in the NPT ensemble for 5000000 steps. The temperature and pressure were kept at 298° K and 1 atm. We used time step of 0.1 fs and the trajectory was sampled every 0.1 ps (1000 step intervals). Total simulation system consisted of 7532 atoms. We analyzed MD trajectory in the context of the angle between phenyl and porphyrin planes ($\theta_{plane-plane}$) and angles relevant for the hydrogen-bonded substrate.

Quantum chemical calculations and auxiliary studies

All quantum chemical calculations were done by means of the DMol^3 [30, 31] software, implemented in Materials Studio 2.2 by Accelrys Inc.: San Diego, CA. Double numerical basis set with polarization functions (denoted as DNP in the software) was used in a combination with GGA PW91 exchange-correlation functional. The accuracy of DFT functionals has been already extensively monitored by many authors [32] also for iron centers in cytochromes [33] and it was shown that the best accuracy should be expected from B3LYP. However, to keep computation time modest we have employed non-HF software. Nevertheless, non-hybrid functionals like BLYP, BP86 or PW91, also give reasonable accuracy with the exception of detailed spin state separations [33, 34]. The calculations were fully unrestricted and the electronic configuration was carefully checked for all stable structures. Transformation mechanism between stable structures was followed by minimum energy pathway calculations based on geometrically selected reaction coordinate (DRC). In this part of the study local exchange-correlation functional VWN was used for calculations following the reaction pathway and only the transition state neighborhood was recalculated with GGA. Final results concerning stabilities of optimized structures and reaction barriers were obtained consistently from PW91 energies. The electronic occupations along the reaction pathways were allowed to smear within 0.01 au window around the Fermi level with full control of total spin not only to avoid convergence problems but also to partly account for prospective multiconfigurational character of the wavefunction. Tentative reaction coordinate for each step of the reaction was defined as the distance between the relevant atom of the substrate origin and the target atom. Formation of the σ-complex was controlled by the distance between oxyferryl oxygen and the C4 carbon of the substrate **1**. The two consecutive processes, proton shuttle and alcohol formation, were simulated by controlling the distance between activated hydrogen and porphyrin nitrogen or oxyferryl oxygen, respectively while the ketone formation was controlled by the distance between the appropriate hydrogen and carbon atoms. Fully optimized final stable structures served as the starting point for the subsequent steps. The model investigated here is large, potential energy profiles in the vicinity of transition states are usually flat while the electronic structure is intricate thus frequency calculations were technically demanding and not always feasible with resources at hand. Frequency calculations were successfully completed only for selected energy barriers (TS2 and TS4). Charges and spin populations were calculated by Hirshfeld and Mulliken population analysis; visualisation and 3D plots were done by Materials Studio package. The effect of protein environment was taken into

account approximately by computing single point energies using conductor-like solvation model COSMO at the GGA-PW91 level [16, 17]. In this model, a cavity around the system is surrounded by a polarizable dielectric continuum. The dielectric constant was set to 5.7, which represented reasonably well the protein environment. The cavity in the dielectric medium was generated using standard van der Waals radii and a solvent probe radius of 2.6 Å.

QM model validation

Even if combined QM/MM methods that can include protein environment in the force field part are nowadays accessible, quantum region remains limited and delicate questions of protonation machinery and protein-active site charge flow are still difficult to tackle with explicitly. Cpd I, an oxoiron(iv) porphyrin radical cation, is believed to be the catalytically active center in P450s involved in hydroxylation although it has not yet been directly detected because of its high reactivity. There has been indirect evidence for the existence of Cpd I [35–38] from low-temperature crystallography, EPR and Mossbauer parameters [38, 39] but its identification was not definitive. In our former paper [18] we have utilized the gas-phase model of Cpd I, where the selection of the basic electronic state was crucial, being at the same time highly arbitrary. We have followed modeling protocol of Yoshizawa et al. [40–42] and selected FeO^{2+} bound with a protoheme porphyrin radical (taken directly from the crystal structure of P450 3A4 cytochrome) with a $(SCH_3)^-$ distal ligand as the working model of Cpd I. Within assumed model with total charge Q=0, electronic properties of the modeled Cpd I complied with those found by majority of other theoretical work. Ground state was found to be antiferromagnetically coupled doublet, with the quartet positioned only 1 kcal mol^{-1} higher. Schoneboom et al. [39] concluded after calculating EPR and Mossbauer parameters that low-lying doublet and quartet states may become heavily mixed due to SOC and a well-defined ground state multiplicity may loose its meaning. Thus, being fully aware of the limitations of our model calculations we did not attempt to contribute to the discussion on absolute relation between the close-lying electronic states and details of spin distribution among cysteinate ligand and porphyrin ring in isolated Cpd I. Indeed, our recent complementary studies on the electronic states of Cpd I with CASPT2 methodology [34] indicate that the ground state of Cpd I may be properly described only by a multiconfiguration wave function. For that purpose the model had to be reasonably reduced by cutting heme side chains. For complementary study on reaction steps originating with parallel conformation of the σ-complex we also used the reduced model (*vide infra*). Preliminary CASSCF investigation of Cpd I corroborate

peculiarities of its antiferromagnetically coupled doublet electronic state with delicate balance between configurations with radical centered either on porphyrin or on cysteine. Only after including dynamical correlation within PT2 scheme the porphyrin-centered doublet becomes the candidate for the ground state, in accord with experimental predictions and our DFT results. It is notable that correlated CASPT2 QM calculations give credence to DFT results validating usefulness of DFT methodology for the system under consideration. The inspection of DFT spin distribution in a precursor complex and in a σ-complex [18] indicates that the doublet of three unpaired electrons parentage is transformed to the one with one unpaired electron in the rate determining step. Thus in the following we assume conventional doublet potential energy surface for the σ-complex and pursue consecutive reaction steps along low-spin route. Prospective influence of the reduction of the model on consecutive reaction profiles was checked by inspecting stabilities and properties of both conformations of a σ-complex utilized in the further study. We have found that the energies were only uniformly shifted down by ca. 3 kcal mol^{-1} by reducing the model while geometrical parameters, spin densities and charge distribution remained virtually unchanged. Therefore for the study of parallel conformation reduced model examined by advanced CASPT2 methodology was used.

Results and discussion

The proposed general mechanism for the σ-complex transformation into oxidized products is shown in Fig. 2. Since the two conformations of the σ-complex emerge from the gas-phase modeling (see Fig. 3) we will discuss the results for the oxidation pathway separately for the two initial structures. Similar two conformations of the reactive complex between Cpd I and benzene were reported in the literature [19–21]; our preliminary DFT study on the insertion of FeO^+ into C-H bond in benzene derivatives endorse also the existence of two stable conformers of reactive σ-complex. Figure 3 shows geometries of σ-complexes for the reduced model optimized with perpendicular (a) or parallel (b) orientation. Table 1 shows the energy difference between parallel and perpendicular conformation with respect to the orientation of phenyl and porphyrin planes. There is no significant difference in the binding energy of the two structures. In gas phase, parallel conformation is by 0.87 kcal mol^{-1} more stable than the perpendicular one while in solvent (PCM model of the protein) the difference is reduced to 0.71 kcal mol^{-1}. This energy difference does not allow for firm discrimination of the two structures. Therefore we aided the QM study with analyses of MD trajectories for the full model embedded in
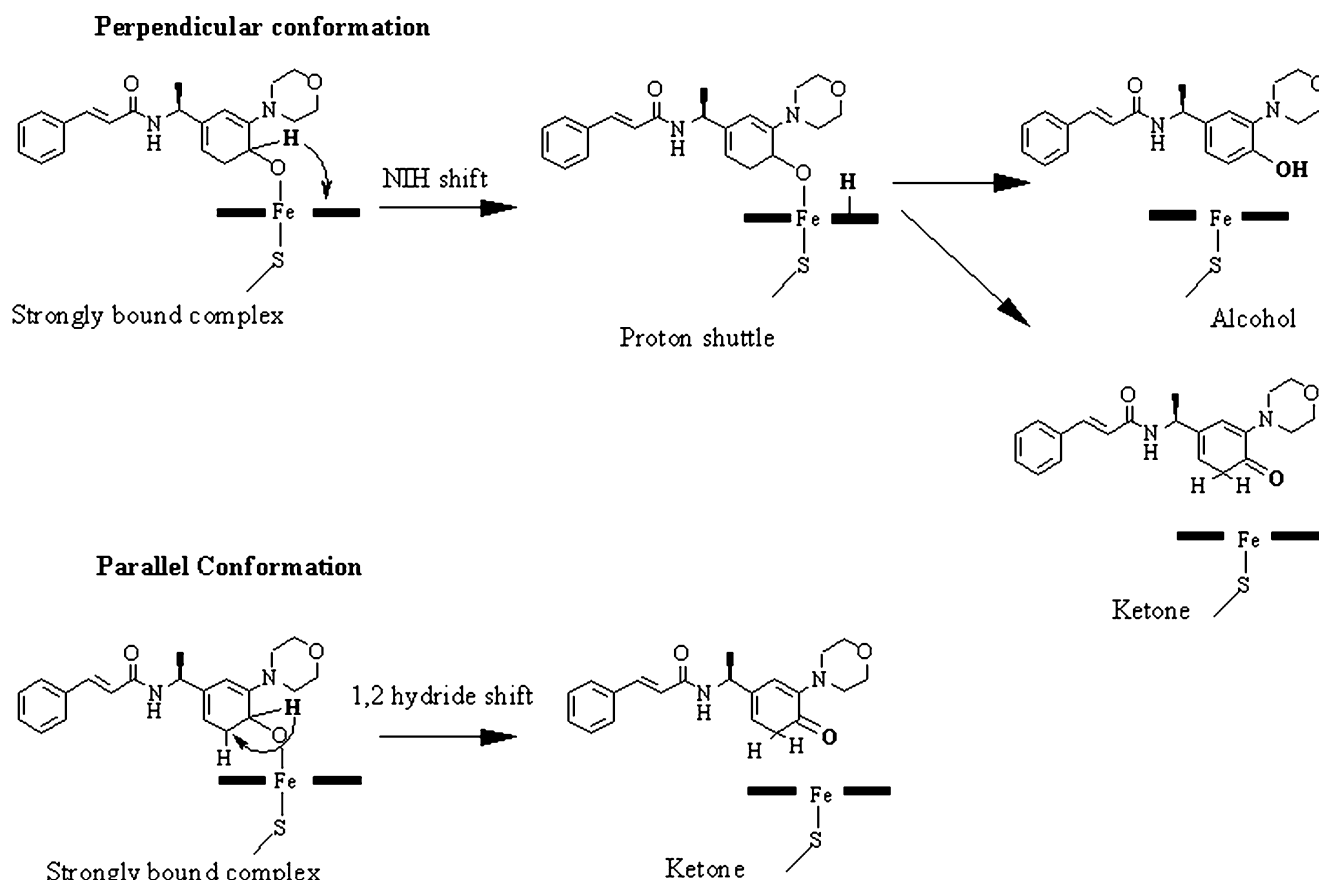
Fig. 2 Proposed mechanisms for σ-complex transformation into oxidized products in metabolism of **1**

the target protein. Qualitative analysis of MD results for the encounter complex between substrate **1** and oxyferryl active center in CYP3A4 is shown in Table 2. It can be seen that the Fe-O-H7 angle remains preferentially within the range of 140–180°. Average distance between O and H7 is 3.26 Å while average angle O-H7-C4 is 141°. The angle between phenyl and porphyrin planes falls in three categories: 56–80° (17%), 80–100° (63%) and over 100° (20%). From this observation it can be inferred that the phenyl ring remains preferentially perpendicular to the porphyrin plane during simulation. Hence perpendicular conformation of the σ-complex should be more probable in CYP3A4 environment, stabilized by hydrophobic interactions of phenylacrylamide chain.

Table 3 shows geometrical parameters of stable structures found by DFT calculations along the reaction route of Cpd I with substrate **1** while Table 4 shows the charges and spin densities along the transformation pathways. Figures 4 and 5 summarize energetic and geometrical features for reaction pathways initiated from the two conformations. For comparative purpose, zero energy level in both Figures is set to the energy of appropriate σ-complex. In both σ-complexes, the substrate bears positive charge of over 0.8 e while charge on porphyrin is negative and spin density is

almost negligible. These observations corroborate carbocationic character of the σ-complex and overall cationic reaction route.

Perpendicular conformation of σ-bonded complex

Proton shuttle (the formation of protonated porphyrin intermediate from the σ-complex) seems to be facilitated in this geometry by exposing the ipso hydrogen toward porphyrin nitrogen (see Fig. 3a). The distance between positively charged ipso hydrogen (Q_H=0.18) and negatively charged porphyrin nitrogen is 2.04 Å. Therefore this distance was used as a natural reaction coordinate to calculate potential energy profile for the formation of proton shuttle intermediate. The energy barrier was found to be 2.84 and 3.64 kcal mol^{-1} in gas and solvent phase, respectively (Table 5, Fig. 4). In the transition state the N-H7 and C4-H7 distances are 1.64 and 1.23 Å while Q_H increases to 0.23. Transition state could not be confirmed here by frequency calculation due to flatness of potential energy surface. In a proton shuttle intermediate, porphyrin accepts the proton charged with +0.34. The carbon-oxygen distance shortens to 1.30 Å while the distance between carbon and morpholine nitrogen becomes 1.38 Å what indicates the change in
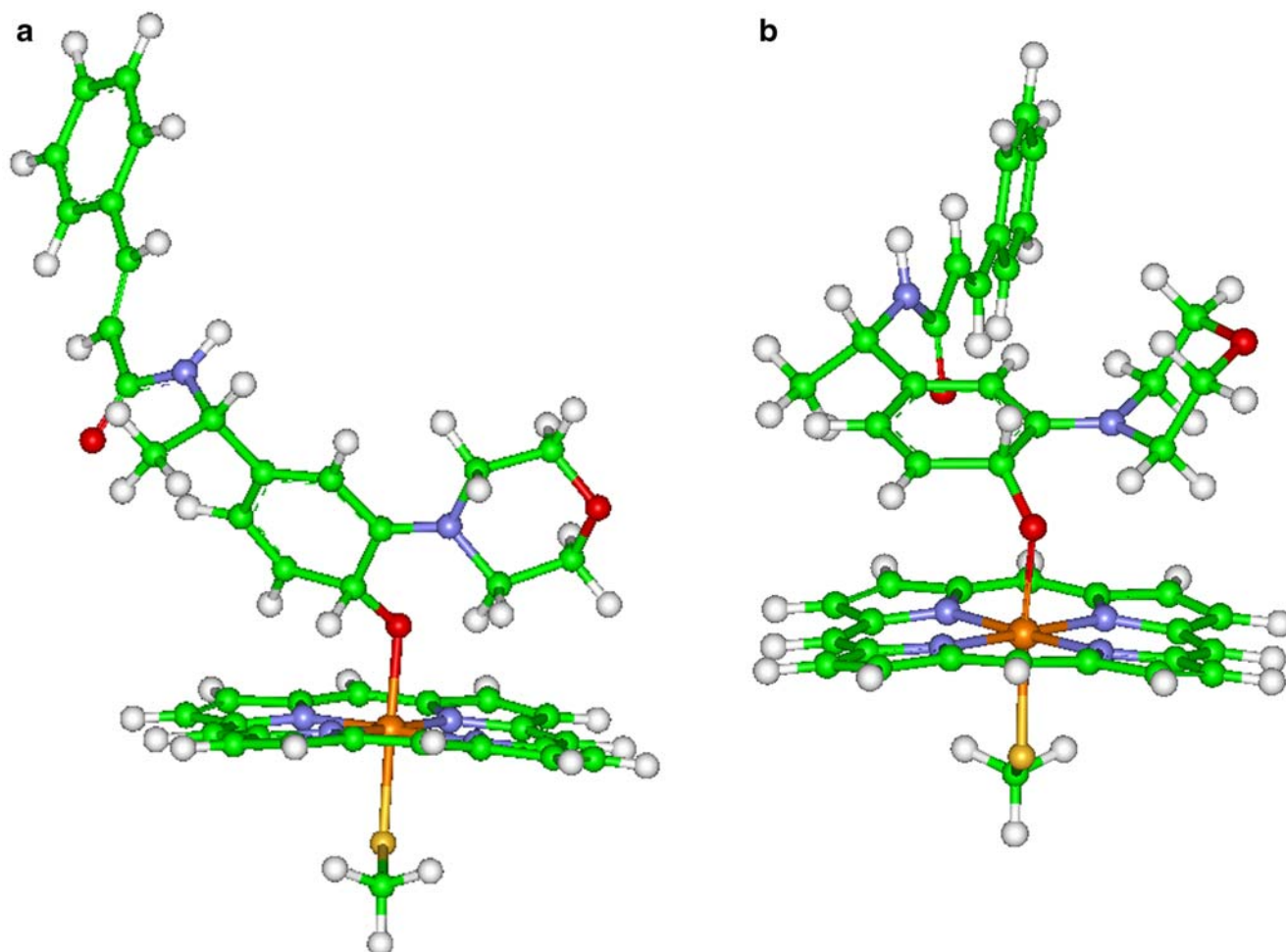
Fig. 3 Optimized structures for two σ-complexes (for reduced model): perpendicular (**a**) and parallel (**b**) orientation of phenyl ring toward porphyrin plane

double bonds conjugation pattern and release of C3-N bond towards its normal, single bond length.

As shown in Fig. 6, porphyrin ring is highly deviated from its native, flat conformation. In this conformation, N-H7 distance is 1.06 Å, O-H7 is 2.27 Å while C5-H7 distance is 1.97 Å. Geometrical parameters suggest that the protonated porphyrin can shuttle hydrogen back forming either alcohol or ketone product with comparable probabilities. In a proton shuttle complex, charge on H7 is 0.34, the charge on oxygen is −0.507, while on C5 carbon it is −0.141. This might indicate the priority for hydrogen shift to more negatively charged oxygen. Indeed, the formation of alcohol meets only a

negligible barrier, corresponding to the rotation with respect to Fe-O-C plane. Transition state for alcohol formation was confirmed by frequency calculation at LDA level, with one imaginary frequency found at 87.2 i cm^{-1}. However, single point GGA calculations produced negative value of the barrier. Exceptionally low energy barrier for alcohol formation has been also observed in previous studies [19–21]. Early transition state is located at O-H7 distance of 1.78 Å, and almost unaltered N-H distance. After forming the alcohol precursor, the hydroxylated substrate becomes nearly neutral and phenyl ring restores fully aromatic structure.

Table 1 Relative energies (with respect to isolated subsystems) for perpendicular and parallel conformation of σ-complex (kcal mol^{-1}, for the reduced model)

	GGA		GGA (COSMO)	
	Perpend.	Parallel	Perpend.	Parallel
Relative energy	−26.09	−26.96	−22.80	−23.50

Table 2 Qualitative analysis of the molecular dynamics trajectory for CYP3A4 bound substrate **1**

	Fe-O-H7	Fe-O-H$_{mor}$	O-H7-C4	O-H$_{mor}$-C$_{mor}$
A	30	99.7	48	4
B	70	0.3	52	96
Average (°)	144.5	112.1	141.0	158.6

Classes A and B denote the probability of sampling a snapshot with angles within ranges: A) below 140° and B) 140 to 180°.

Table 3 Geometrical parameters of stationary structures for the reaction of Cpd I with substrate **1** (all distances in Å)

Structure	Fe-O	O-C_4	C_4-H_7	N_{por}-H_7	H_7-O	C_5-H_7	C_4-C_5	C-N_{mor}
Perpendicular conformation								
σ-complex	1.96	1.35	1.16	2.04	2.04	1.99	1.48	1.34
TS1	2.02	1.35	1.23	1.64	1.98	2.05	1.47	1.35
Proton shuttle	1.96	1.30	2.13	1.06	2.27	1.97	1.41	1.38
TS2	2.12	1.32	2.23	1.06	1.78	2.48	1.42	1.40
Alcohol	2.74	1.38	1.93	2.18	0.98	2.43	1.40	1.41
TS3	2.07	1.28	2.09	1.33	2.46	1.42	1.45	1.40
Ketone	2.17	1.25	2.71	2.73	2.71	1.11	1.50	1.40
Parallel conformation								
σ-complex	2.01	1.37	1.14	4.31	2.03	2.02	1.50	1.34
TS4	2.04	1.29	1.30	4.00	2.16	1.46	1.46	1.35
ketone	2.16	1.25	2.10	3.09	2.69	1.11	1.50	1.39

Proton shuttle intermediate may also transfer the hydrogen to ortho carbon (C5) to give ketone product. Energy barrier for ketone formation was located at 7 kcal mol^{-1} in gas phase while in the solvent it was increased to 7.42 kcal mol^{-1}. Transition state is characterized by the distances: N-H7 of 1.33 Å, C5-H7 of 1.42 Å and C4-O of 1.28 Å (Table 3). In stable ketone product, C4-C5 distance is 1.50 Å and the distance between C and morpholine N becomes 1.40 Å, characteristic for regular single bonds.

Ketone formation from parallel conformation

Already brief inspection of geometrical parameters of the σ-complex in parallel conformation excludes the possibility of the reaction pathway via proton shuttle intermediate as the activated hydrogen points out in the direction opposite to a porphyrin plane (see Fig. 3b). In this case the only viable mechanism of the arene oxidation remains intramolecular migration of the hydrogen from the site of oxidation to the adjacent carbon termed the 1,2 hydride shift. We have modeled this reaction step by sampling the C5-H7 distance to control the transfer of hydrogen from tetrahedral carbon to ortho carbon (C5) to give ketone product (1,2 hydride shift). Figure 6 summarizes essential features for ketone formation starting from parallel σ-complex between substrate **1** and Cpd I. Transition state is achieved at C5-H7 and C4-H7 distances of 1.46 and 1.30 Å, respectively C4-O distance of 1.29 Å. Energy barrier for ketone formation was found to be 7.93 kcal mol^{-1} in gas phase and 7.77 kcal mol^{-1} in solvent phase (Table 5). Transition state was confirmed by frequency calculation with one imaginary frequency found at 976 i cm^{-1}, with clear corresponding eigenvector. The energy barrier is comparable to the previously discussed energy barrier for ketone formation starting from proton shuttle that was in accord with other results [19]. In our case we have not found low-barrier ketone formation by 1,2 hydride shift in parallel configuration reported in [21]. However, even if such nearly barrierless process should be possible here, lower probability of achieving parallel configuration for the substrate bound in CYP3A4 enzyme would make this reaction route less probable.

Table 4 Group Mulliken charges and group spin densities of stationary structures

Structure	Fe		O		Porphyrin		Substrate	
	Charge	Spin	Charge	Spin	Charge	Spin	Charge	Spin
Perpendicular conformation								
σ-complex	0.20	0.79	−0.59	0.03	−0.47	−0.06	0.87	0.01
TS1	0.20	0.76	−0.57	0.03	−0.40	−0.07	0.80	0.00
Proton shuttle	0.18	0.63	−0.53	0.04	−0.17	−0.05	0.54	0.08
TS2	0.17	0.58	−0.58	0.05	−0.17	−0.03	0.23	0.11
Alcohol	0.19	0.77	−0.47	0.00	−0.33	−0.03	0.09	0.01
TS3	0.17	0.72	−0.48	0.01	−0.21	−0.06	0.52	0.02
Ketone	0.18	0.74	−0.39	0.00	−0.43	−0.05	0.22	0.00
Parallel conformation								
σ-complex	0.21	0.81	−0.56	0.03	−0.44	−0.06	0.81	0.04
TS4	0.10	0.73	−0.51	0.01	−0.39	−0.05	0.77	0.01
Ketone	0.18	0.74	−0.40	0.00	−0.43	−0.05	0.22	0.00

Fig. 4 Potential energy profile for the formation of alcohol and/or ketone product from perpendicular orientation of σ-complex mediated by proton shuttle (full model, energies relative to σ-complex in kcal mol^{-1}, COSMO values in parentheses); next to transition state geometries, charges on substrate and porphyrin and critical distances (in Å) are shown
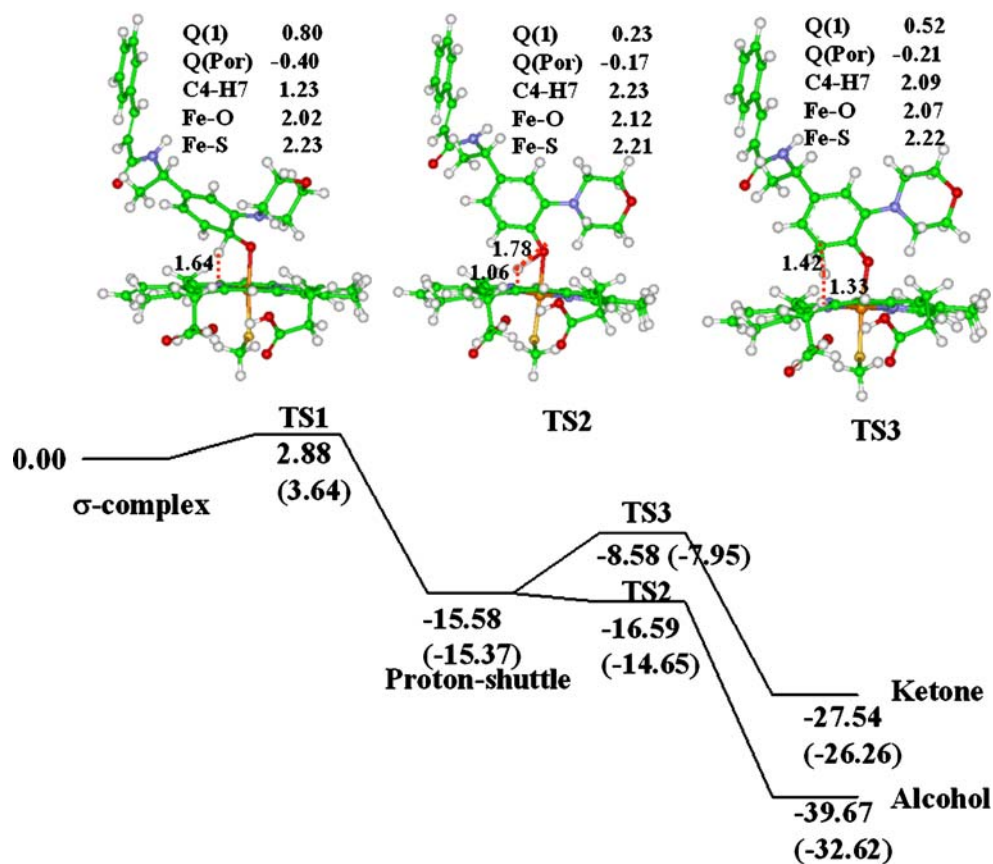

Fig. 5 Potential energy profile for the formation of ketone product from parallel orientation of σ-complex (reduced model, energies relative to σ-complex in kcal mol^{-1}, COSMO values in parentheses). Next to optimized geometries for stationary structures charges on substrate and porphyrin and critical distances (in Å) are shown
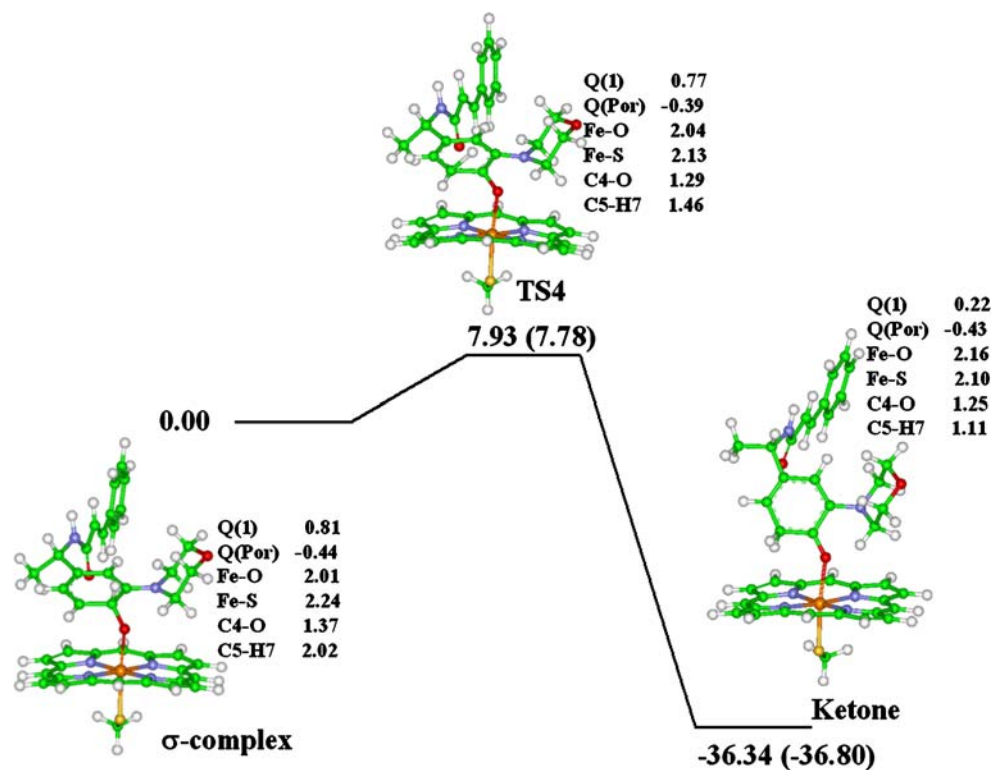
Table 5 Relative energies (with respect to σ-complex, kcal mol^{-1}) and energy barriers for the oxidation of substrate **1** by Cpd I

Structure	Relative energy		Energy barrier	
	Gas phase	COSMO	Gas phase	COSMO
Perpendicular conformation				
σ-complex	0.00	0.00		
TS1	2.88	3.64	2.88	3.64
Proton shuttle	−15.58	−15.37		
TS2	−16.59	−14.65	−1.02	0.72
Alcohol	−39.67	−32.62		
TS3	−8.58	−7.95	7.00	7.42
Ketone	−27.54	−26.26		
Parallel conformation				
σ-complex	0.00	0.00		
TS4	7.93	7.78	7.93	7.77
Ketone	−36.34	−36.80		

Conclusion

Cytochrome P450 mediated metabolism of (S)-N-[1-(3-morpholin-4ylphenyl)ethyl]-3-phenylacrylamide was investigated using density functional theory. Two different orientations for the phenyl ring of the substrate with respect
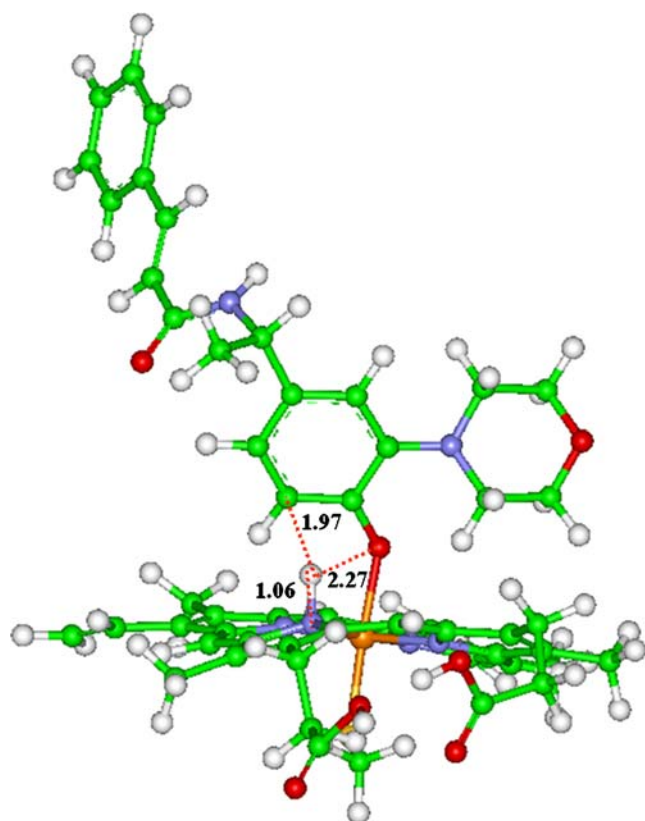

Fig. 6 Optimized structure of proton shuttle intermediate. Distances are shown in Å

to porphyrin plane were studied. In accord with previous studies, first step of the aromatic hydroxylation occurs through electrophilic attack of phenyl ring to form reactive σ-complex. Addition of Cpd I to the substrate is the rate determining step and other steps proceed with relatively low energy barrier. Reaction proceeds predominantly via cationic pathway on doublet potential energy surface. In variance with model benzene studies, however, the existence of bulky substituents, influencing also electronic structure, modifies greatly energetic and structural features of the metabolism. Already in our previous paper [18] we showed the importance of morpholinyl fragment in ortho position to the oxidized site via providing electron-reach and conformationally flexible nitrogen what significantly lowers the barrier for the rate determining step. Here we present the results for consecutive reaction steps leading to the oxidized product where the mechanism obviously depends on spatial positioning of the substrate in enzymatic reaction cavity. The overall reaction pattern proceeds along energetic profile over 20 kcal mol^{-1} below that postulated for benzene (see Table 5). Already strongly bound σ-complex is stabilized by 26 kcal mol^{-1} with respect to isolated Cpd I and substrate **1**, which shifts all stationary structures, including transition states below the limit of isolated subsystems. To add credence to this finding we have utilized simple model DFT calculations for the interaction between FeO^+ molecular cation and benzene, aminobenzene and 3-methylaminobenzene molecules. At the GGA level and sextet potential energy surface stabilization energies of the σ-complex between oxygen and phenyl moiety, analogous to that found for substrate **1**, were −25.5, −51.7 and −62.3 kcal mol^{-1} for benzene, aniline and 3-methylaniline, respectively. This result validates the increase of the σ-complex stability by the substituents in ortho and para positions with respect to tetrahedral carbon in substrate **1**.

No significant difference in energy and electronic structure between parallel and perpendicular phenyl orientation toward the porphyrin plane was found by DFT calculations either for the gas phase model or for PCM solvent model. However, auxiliary molecular dynamics simulations for full enzyme model helped to discriminate the orientations of phenyl plane and indicated the perpendicular orientation as a favorable one. Hence we postulate that in CYP3A4 environment phenyl ring of the studied substrate should remain preferentially perpendicular with respect to porphyrin plane during the metabolism. Perpendicular orientation of phenyl ring in σ-complex imposes consecutive protonated porphyrin intermediate (proton-shuttle), which further may produce alcohol or ketone products. Alcohol is the major product as the energy barrier for alcohol formation is almost negligible. Strongly bound σ-complex with parallel conformation leads solely to

ketone product due to steric constraints but is disfavored by enforced substrate configuration. This in turn highly favors the formation of hydroxylated product for substrate **1** metabolized by the oxyferryl active site in CYP3A4.

References

1. Rendic S, Di Carlo FJ (1997) Drug Metab Rev 29:413–580
2. Kumar GN, Surapaneni S (2001) Med Res Rev 21:397–411
3. Guengerich FP (2001) Chem Res Toxicol 14:611–650
4. Anzenbacher P, Anzenbacherova E (2001) Cell Mol Life Sci 58:737–747
5. Ekins S, Bravi G, Binkley S, Gillespie JS, Ring BJ, Wikel JH, Wrighton SA (1999) J Pharmacol Exp Ther 290:429–438
6. Lewis DF, Lake BG (1998) Toxicology 125:31–44
7. Wu YJ, Boissard CG, Greco C, Gribkoff VK, Harden DG, He H, L'Heureux A, Kang SH, Kinney GG, Knox RJ, Natale J, Newton AE, Lehtinen-Oboma S, Sinz MW, Sivarao DV, Starrett JE Jr, Sun L, Tertyshnikova S, Thompson MW, Weaver D, Wong HS, Zhang L, Dworetzky SI (2003) J Med Chem 46:3197–3200
8. Wu YJ, Davis CD, Dworetzky S, Fitzpatrick WC, Harden D, He H, Knox RJ, Newton AE, Philip T, Polson C, Sivarao DV, Sun L, Tertyshnikova S, Weaver D, Yeola S, Zoeckler M, Sinz MW (2003) J Med Chem 46:3778–3781
9. Williams PA, Cosme J, Vinkovic DM, Ward A, Angove HC, Day PJ, Vonrhein C, Tickle IJ, Jhoti H (2004) Science 305:683–686
10. Yano JK, Wester MR, Schoch GA, Griffin KJ, Stout CD, Johnson EF (2004) J Biol Chem 279:38091–38094
11. Ekroos M, Sjogren T (2006) Proc Natl Acad Sci USA 103:13682–13687
12. Sono M, Roach MP, Coulter ED, Dawson JH (1996) Chem Rev 96:2841–2888
13. Denisov IG, Makris TM, Sligar SG, Schlichting I (2005) Chem Rev 105:2253–2278
14. Shaik S, Kumar D, de Visser SP, Altun A, Thiel W (2005) Chem Rev 105:2279–2328
15. Ortiz de Montellano PR, De Voss JJ (2002) Nat Prod Rep 19:477–493
16. Klamt A, Schüürmann G (1993) J Chem Soc Perkin Trans 2:799–805
17. Klamt A, Jonas V, Burger T, Lohrenz J (1998) J Phys Chem A 102:5074–5085
18. Shaikh AR, Broclawik E, Ismael M, Tsuboi H, Koyama M, Kubo M, Del Carpio CA, Miyamoto A (2006) Chem Phys Lett 419:523–527
19. Visser SP, Shaik S (2003) J Am Chem Soc 125:7413–7424
20. Bathelt CM, Ridder L, Mulholland AJ, Harvey JN (2003) J Am Chem Soc 125:15004–15005
21. Bathelt CM, Lars Ridder L, Mulholland AJ, Harvey JN (2004) Org Biomol Chem 2:2998–3005
22. Luty BA, Wasserman ZR, Stouten PFW, Hodge CN, Zacharias M, McCammon JA (1995) J Comput Chem 16:454–464
23. Pattabiraman N, Levitt M, Ferrin TE, Langridge R (1985) J Comput Chem 6:432–436
24. Meng EC, Shoichet BK, Kuntz ID (1992) J Comput Chem 13:505–524
25. Paulsen MD, Ornstein RL (1991) Proteins 11:184–204
26. Endou A, Teraishi K, Yajima K, Yoshizawa K, Ohashi N, Takami S, Kubo M, Miyamoto A, Broclawik E (2000) Jpn J Appl Phys 39:4255–4260
27. Onozu T, Miura R, Takami S, Kubo M, Miyamoto A, Iyechika Y, Maeda T (2000) Jpn J Appl Phys 39:4400–4403
28. Onozu T, Gunji I, Miura R, Ammal SSC, Kubo M, Teraishi K, Miyamoto A, Iyechika Y, Maeda T (1999) Jpn J Appl Phys 38:2544–2548
29. Koyama M, Hayakawa J, Onodera T, Ito K, Tsuboi H, Endou A, Kubo M, Del Carpio CA, Miyamoto A (2006) J Phys Chem B 110:17507–17511
30. Delley B (1990) J Chem Phys 92:508–517
31. Delley B (2000) J Chem Phys 113:7756–7769
32. Lundberg M, Siegbahn PEM (2005) J Comput Chem DOI 1002/jcc.2026
33. Pierloot K, private communication
34. Radon M, Broclawik E, J Chem Theory Comput (in press)
35. Dowers TS, Rock DA, Jones JP (2004) J Am Chem Soc 126:8868–8869
36. Schlichting I, Berendzen J, Chu K, Stock AM, Maves SA, Benson DE, Sweet RM, Ringe D, Petsko GA, Sligar SG (2000) Science 287:1615–1622
37. Kaizer J, Klinker EJ, Oh NY, Rohde JU, Song WJ, Stubna A, Kim J, Munck E, Nam W, Que L Jr (2004) J Am Chem Soc 126:472–473
38. Davydov R, Makris TM, Kofman V, Werst DE, Sligar SG, Hoffman BM (2001) J Am Chem Soc 123:1403–1453
39. Schoneboom JC, Niese F, Thiel W (2005) J Am Chem Soc 127:5840–5853
40. Yoshizawa K (2002) Coord Chem Rev 226:251–259
41. Kamachi T, Yoshizawa K (2003) J Am Chem Soc 125:4652–4661
42. Kamachi T, Shestakov AF, Yoshizawa K (2004) J Am Chem Soc 126:3672–3673